Simple and efficient generation of gap solitons in Bose-Einstein condensates

Michał Matuszewski,[1,2] Wieslaw Królikowski,[2] Marek Trippenbach,[1,3] and Yuri S. Kivshar[4]
[1]*Institute for Theoretical Physics, Warsaw University, Hoża 69, PL-00-681 Warsaw, Poland*
[2]*Laser Physics Centre, Research School of Physical Sciences and Engineering, Australian National University, Canberra, Australian Capital Territory 0200, Australia*
[3]*Soltan Institute for Nuclear Studies, Hoża 69, PL-00-681 Warsaw, Poland*
[4]*Nonlinear Physics Centre and ARC Centre of Excellence for Quantum-Atom Optics, Research School of Physical Sciences and Engineering, Australian National University, Canberra, Australian Capital Territory 0200, Australia*
(Received 28 December 2005; published 27 June 2006)

We suggest an efficient method for generating matter-wave gap solitons in a repulsive Bose-Einstein condensate, when the gap soliton is formed from a condensate cloud in a harmonic trap after turning on a one-dimensional optical lattice. We demonstrate numerically that this approach does not require preparing the initial atomic wave packet in a specific state corresponding to the edge of the Brillouin zone of the spectrum, and losses that occur during the soliton generation process can be suppressed by an appropriate adiabatic switching of the optical lattice.

DOI: 10.1103/PhysRevA.73.063621 PACS number(s): 03.75.Lm, 05.45.Yv

I. INTRODUCTION

Recent experimental developments in the fields of nonlinear optics and Bose-Einstein condensation provide unique opportunities for the studies of many nonlinear phenomena. Moreover, due to a formal similarity of the Gross-Pitaevskii equation for the dynamics of matter waves and the nonlinear Schrödinger equation for light propagating in a nonlinear Kerr medium, it is possible to interchange and transfer many interesting ideas between these two fields. One of them is the generation of nonspreading localized wave packets usually called *optical solitons* or *matter-wave solitons* [1].

Bright solitons, which are quite common objects in different problems of nonlinear optics, have been only recently demonstrated in two independent experiments with matter waves [2,3]. In this case, the wave-packet spreading due to dispersion is compensated by an attractive interaction between atoms. Both optical and matter-wave solitons can also be formed due to an interplay between nonlinearity and periodicity [4–6].

In optics, the presence of a periodically varying refractive index of a medium results in a band-gap structure of the transmission spectrum of light. This subsequently affects the propagation of optical beams (pulses), which is determined by the diffraction (dispersion) curves of the transmission bands and forbidden gaps of the wave spectrum. It was demonstrated that periodic structures can modify dramatically the wave diffraction [7], and therefore they introduce a novel way for controlling self-action of light in nonlinear periodic media [8,9]. In particular, if the refractive index decreases increasing light intensity due to a nonlinearity-induced response of the material, the beam normally experiences broadening due to self-defocusing. However, in periodic photonic structures, the same type of defocusing nonlinearity can lead to the beam localization [10]. For deep periodic modulations, this effect should result in the formation of discrete solitons. Indeed, as was shown both numerically and experimentally in Ref. [11], increasing the depth of the refractive index modulation leads to a sharp crossover between the continuous and discrete properties of the lattice. It is manifested in a specific type of light localization and gap-soliton generation which become possible for a self-defocusing medium only in case of a discrete model.

An analogous effect of the gap-soliton generation in the regime of repulsive interaction was observed for Bose-Einstein condensates. This first experimental observation [12] was reported for ^{87}Rb atoms in a weak optical lattice. In this case, the anomalous dispersion of the atomic cloud is realized at the edge of the Brillouin zone; if the coherent atomic wave packet is prepared in the corresponding state, a matter-wave gap soliton is formed inside the spectral gap. However, it took a considerable experimental effort to generate the initial state of the Bose-Einstein condensate in a proper way, by introducing an acceleration to the optical lattice and other tricks [12,13].

In this paper, we reveal that the matter-wave gap solitons can be generated by a simpler and straightforward method that allows creation of stable, long-lived gap solitons of a repulsive Bose-Einstein condensate in a one-dimensional optical lattice. In our scenario, the gap soliton is formed from an initial ground state of a harmonic trap after turning on the optical lattice, due to the cloud relaxation, rather than as a result of preparing the initial atomic wave packet at a certain point of the band-gap structure. In addition, we demonstrate that losses during this process can be suppressed by an appropriate adiabatic switching of the optical lattice.

The paper is organized as follows. In Sec. II we introduce our theoretical model. Then, in Sec. III we present two methods for generating the matter-wave gap solitons and demonstrate their efficiency in numerical simulations. The coupled-mode theory for describing the self-trapping mechanism is introduced in Sec. IV where we discuss the essential physics of the localization process. Finally, Sec. V concludes the paper.

II. THEORETICAL MODEL

We analyze our matter-wave system in the framework of the three-dimensional mean-field Gross-Pitaevskii equation

for the macroscopic wave function $\Psi(\mathbf{r},t)$, written in the standard form

$$i\hbar\frac{\partial\Psi}{\partial t}=\left(-\frac{\hbar^2}{2m}\Delta+U(\mathbf{r},t)+\frac{4\pi a\hbar^2}{m}|\Psi|^2\right)\Psi, \qquad (1)$$

where for the repulsive condensate the scattering length is positive ($a>0$). We assume that the external potential $U(\mathbf{r},t)$ consists of two parts, a harmonic trap and a one-dimensional optical lattice, i.e.,

$$U(\mathbf{r},t)=f_1(t)\varepsilon\,\sin^2\left(\frac{\pi z}{d}\right)+\frac{m}{2}[\omega_\perp^2\varrho^2+f_2(t)\omega_z^2z^2],$$

where $d=\lambda/2$ is the period of the optical lattice potential, $\rho=(x^2+y^2)^{1/2}$ is the two-dimensional radial coordinate, and the cylindrically symmetric harmonic trap is characterized by the longitudinal and transverse frequencies ω_z and $\omega_\perp$, respectively. We also introduce the depth ε and period λ of an optical lattice. Temporal variations of the potential are described by two functions $f_1(t)$ and $f_2(t)$, which account for the adiabatic processes of turning off the longitudinal part of the harmonic trap and turning on the optical lattice over the stationary condensate. More details about this tuning will follow in the next section.

In our numerical calculations, we use both three-dimensional model and (more often) quasi-one-dimensional reduced model, in which we assume that the transverse harmonic confinement is so tight that no transverse excitations occur [14,15]. As a result of this assumption, the three-dimensional wave function resembles the transverse ground state of a harmonic potential in the transverse cross section, and the nonlinear dynamics can be described by a one-dimensional Gross-Pitaevskii equation after rescaling the nonlinear coefficient $a_{1D}=(m\omega_\perp/2\pi\hbar)a$.

III. NUMERICAL RESULTS AND DISCUSSIONS

In our numerical simulations, we suggest and analyze systematically two methods for generating matter-wave gap solitons in the repulsive Bose-Einstein condensates loaded in a shallow one-dimensional optical lattice.

A. The first method

In the first method, we start from the ^{87}Rb condensate (atomic mass 86.9 amu and scattering length 5.3×10^{-9} m) as an eigenstate of a cylindrically symmetric harmonic trap with the frequencies $\omega_{z0}=2\pi\times40$ Hz and $\omega_\perp=2\pi\times50$ Hz. Then we instantaneously turn off the longitudinal trapping potential leaving the perpendicular harmonic potential on and simultaneously switch on, in the same direction, a one-dimensional optical lattice with the spatial period $\lambda=30$ μm. For this lattice we define the recoil energy $E_{\text{recoil}}=\hbar^2(2\pi/\lambda)^2/(2m)$. Such a lattice can be created by interfering two laser beams propagating at a small angle [9,16]. For the wavelength of 783 nm, used in Ref. [12], this angle would be equal to 2.3°. After an abrupt change of the potential, a quasi-one-dimensional dynamics takes place, in which atoms slowly tunnel to the neighboring lattice sites, while the confinement in the direction perpendicular to the optical lattice remains unaffected. As is shown in Figs. 1(a)–1(c), depending on the initial number of atoms, we observe asymptotically either expansion of the condensate over more and more lattice sites [see Fig. 1(b)] or condensate stabilization accompanied by the formation of a spatially localized state occupying just a few lattice sites [see Fig. 1(c)]. We checked that there exists a threshold in the initial number of atoms (with all the rest of the system parameters fixed) above which a stable spatially localized state is generated in the optical lattice.

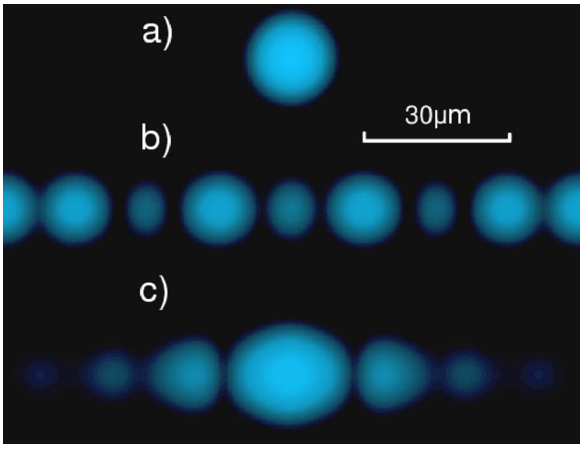

FIG. 1. (Color online) Generation of a matter-wave gap soliton. Shown are the density snapshots for (a), (b) $N=200$ atoms at the input ($t=0$) and after expansion ($t=0.4$ s), respectively, and (c) $N=500$ atoms, after expansion at $t=1.4$ s. The lattice parameters are $\varepsilon=2.3E_{\text{recoil}}$ and period 15 μm.

These results are summarized in Figs. 2(a)–2(c), where we show the profile of the soliton wave function and the

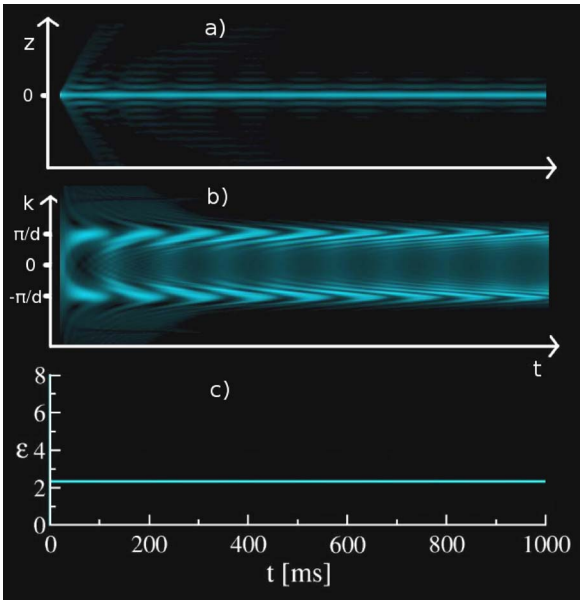

FIG. 2. (Color online) (a) Temporal evolution (from left to right) of the axial density of the condensate [see Fig. 1(c)]. (b) Evolution shown in the Fourier space. (c) Temporal variation of the depth of the optical lattice (cf. Fig. 5 below).

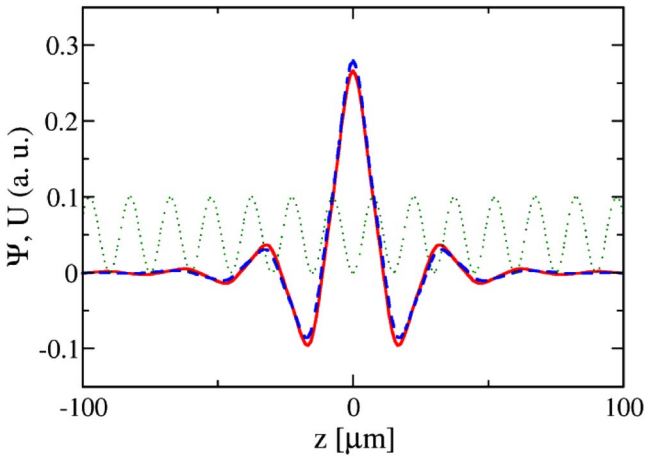

FIG. 3. (Color online) Wave function of the matter-wave gap soliton of Fig. 1(c), as predicted by the one-dimensional Gross-Pitaevskii equation (dashed) and the full three-dimensional model (solid); dotted line shows the lattice potential.

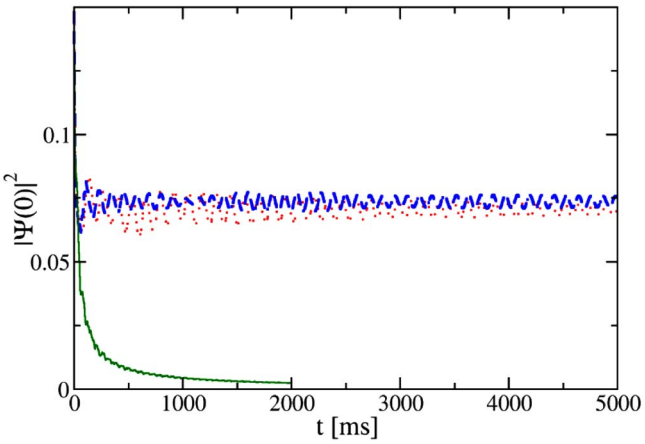

FIG. 4. (Color online) Evolution of the peak amplitude of the atomic cloud in the lattice for (a) $N=$(a) 200 atoms (solid) and (b), (c) 500 atoms in the one-dimensional (dashed) and three-dimensional (dotted, rescaled) models, respectively.

corresponding dynamics in the Fourier space. In the Fourier space, a clear localization at the edges of the first band occurs. To understand the importance and specific features of this localization process, we notice that the evolution of a condensate in a one-dimensional optical lattice can be described within the effective mass approximation

$$i\hbar\frac{\partial\psi}{\partial t} = -\frac{\hbar^2}{2m_{\text{eff}}}\frac{\partial^2\psi}{\partial z^2} + \frac{4\pi a_{\text{eff}}\hbar^2}{m}|\psi|^2\psi, \tag{2}$$

where $\psi(z,t)$ is an envelope of the condensate wave function at the edge of the Brillouin zone of the spectrum. The localized state can be supported only if the sign of the effective mass m_{eff} is opposite to the sign of the scattering length a_{eff}. Since for a repulsive condensate $a_{\text{eff}}>0$, the effective mass in this case has to be negative (anomalous diffraction). This condition is indeed satisfied for the matter waves close to the edge of the Brillouin zone. In Sec. V we present a simple model that allows us to describe this kind of the localization process.

In Fig. 3, we show the wave-function profile for the case of $N=500$ atoms at $t=1.4$ s, when the gap soliton is generated, as shown in Fig. 1(c). The phase structure of the resulting state corresponds to the edge of the first band of the Brillouin zone [17]. In addition, we compare the results obtained from the integration of the one- and fully three-dimensional Gross-Pitaevskii models, and notice that the condensate dynamics looks practically the same in both cases. With good accuracy, we can therefore assume that the condensate remains in the ground state of the transverse harmonic potential that is left on all the time. Also, in Fig. 4 we show the evolution of the peak amplitude of the atomic cloud that fully supports our observation. As mentioned above, for $N=200$ atoms we predict overall spreading of the wave packet and the peak amplitude vanishes gradually. For larger numbers of input atoms (e.g., $N=500$), the numerical simulations of both one- and three-dimensional models show the stabilization effect and both approaches predict almost the same final distribution of atoms on a few neighboring lattice sites. In earlier studies [12,15], the generated gap soliton was unstable due to the excitation of transverse modes of the harmonic trap. Here, we suggest applying an optical lattice with a period comparable to the transverse extent of the condensate. Such a configuration (i.e., a sparser lattice) has a much more favorable ratio of the energies of the transverse and longitudinal modes, and the suppression of the instability is observed.

B. The second method

In the loading scenario discussed above, the key idea was to suddenly replace the harmonic trap in the longitudinal direction with a shallow periodic potential of a one-dimensional optical lattice; in this case, the final state corresponding to a gap soliton is composed of a few hundreds of atoms. Moreover, the matter-wave gap solitons created in this way are very narrow, and they occupy only a few lattice sites. In addition, the loading efficiency is relatively low. For that reason, below we suggest and discuss in detail the other method for generating matter-wave gap solitons. In this second scenario, we propose suddenly replacing the longitudinal harmonic trap with a deep lattice, and then gradually reducing the lattice depth to a certain final value. This kind of condensate dynamics does not leave atoms as much freedom to escape the central region as they had before, so we can achieve higher values of the atomic densities in the soliton. Moreover, by applying this method we can end up with very shallow traps, much below the depth accessible in the first scenario. In Fig. 5, we present the result of our numerical simulations of the one-dimensional model for an adiabatic reduction of the lattice depth from $\varepsilon=8E_{\text{recoil}}$ to E_{recoil}. During this dynamics, the size of the condensate grows considerably due to the strong reduction of the lattice depth. In the simulations shown in Fig. 5, we were able to decrease the lattice depth to a level 2.5 times smaller than in the first method discussed above, and we still obtained a stable state with about 500 atoms. The profile of the corresponding matter-wave gap soliton is presented in Fig. 6, and the no-

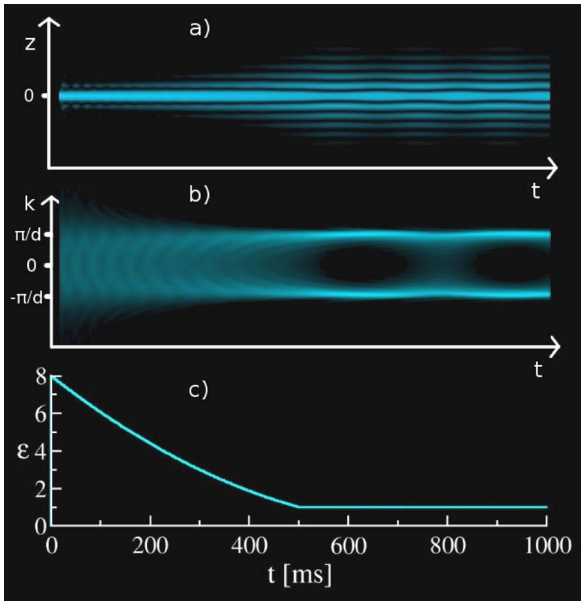

FIG. 5. (Color online) Top: Temporal evolution (from left to right) of the axial density of the condensate in the case of adiabatic reduction of the lattice potential from $\varepsilon=8E_{\mathrm{recoil}}$ to E_{recoil} during the first $t=500$ ms. Middle: Evolution shown in Fourier space. Bottom: Temporal variation of the depth of the optical lattice.

ticeable difference between Figs. 3 and 6 is the width of the created gap soliton. Both gap solitons contain the same total number of atoms but, since in the second method we use a much weaker lattice, the atoms are spread over a much larger region.

To compare the efficiency of these two generation schemes, we perform additional numerical simulations and study how variations of the initial number of atoms and the lattice depth influence the final number of atoms in the matter-wave gap soliton. In Fig. 7, we monitor the efficiency of the soliton generation by counting the atoms that remain after $t=0.5$ s within a window of 200 μm around the central peak. This choice is somewhat arbitrary, but the result does

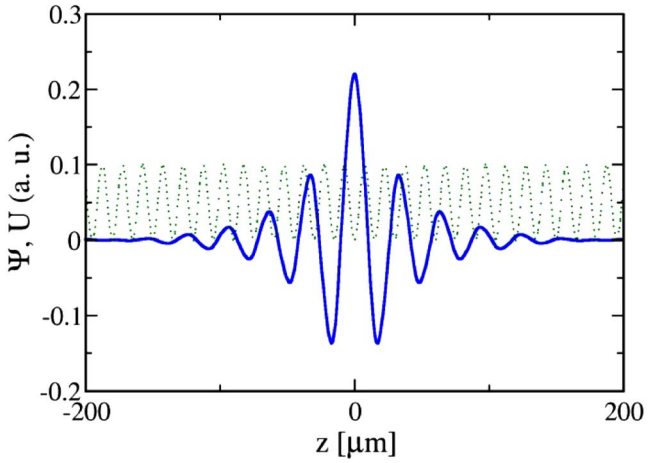

FIG. 6. (Color online) Profile of the condensate wave function at $t=1$ s for the gap soliton generation shown in Fig. 5. Dotted line shows the profile of the optical lattice.

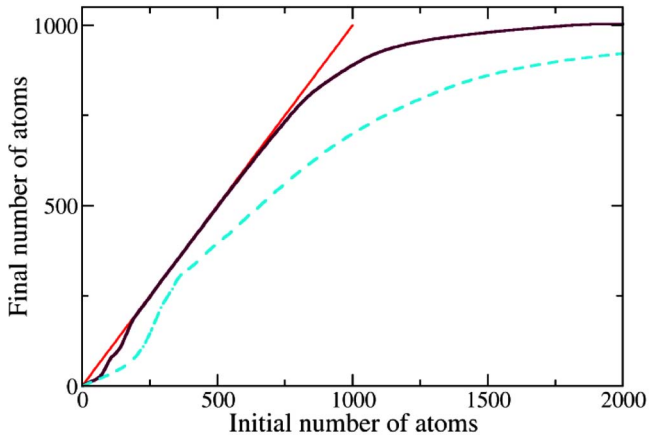

FIG. 7. (Color online) Number of atoms in the window [−100 μm, 100 μm], which is approximately equal to the number of atoms in the generated gap soliton, at $t=500$ ms, as a function of the initial number of atoms. Dashed line corresponds to the scenario with a constant lattice depth of $\varepsilon=2.3E_{\mathrm{recoil}}$, and the solid line to the case of the adiabatic reduction of the lattice potential after switching it on from $\varepsilon=8E_{\mathrm{recoil}}$ to $2.3E_{\mathrm{recoil}}$ during the first 200 ms. Straight line marks the available number of atoms.

not depend qualitatively on the size of the window. We observe that our adiabatic scheme allows us to achieve almost 100% generation efficiency in a broad range of the initial atom number. We also reveal that there exists a limit in the final number of atoms that we can trap into the gap soliton. Both the schemes display saturation above 1000 atoms. We can estimate the maximal number of atoms that can be trapped in the soliton by employing the effective-mass approximation and assuming that the size of the soliton cannot be smaller than one lattice well. Using the parameters given above we estimate the upper limit to be around 1200 atoms, which is almost five times larger than that reported in the first experimental observation [12].

It is clear that the adiabatic scheme enables one to achieve a higher final population, and Fig. 8 shows clearly the advantage of this method. In this figure, we plot the final number of atoms in the gap soliton (we use a similar criterion as discussed above, starting with 500 atoms) as a function of the final value of the optical lattice depth. The adiabatic method leads to a much smaller loss of atoms during the loading process, and it can be used to generate matter-wave gap solitons in much shallower lattices. Solitons generated in this way span quite a large number of lattice sites, and they exhibit much higher mobility, which can be useful for potential applications; see [18]. The latter feature can be seen in Fig. 8, which shows a clear threshold for soliton generation that is more pronounced for the adiabatic approach.

Finally, we comment briefly on the soliton lifetime. In our model and numerical simulations we neglect inelastic losses, so that the time scale at which we follow the soliton generation dynamics remains quite long. Still, we have checked that including inelastic losses does not change our main results significantly, due to low densities of the localized structures generated, but it remains the main factor that will limit the lifetime of gap solitons in real experiments.

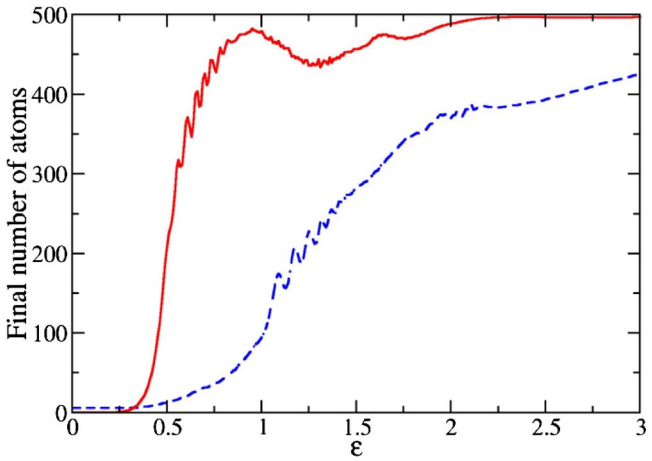

FIG. 8. (Color online) Number of atoms in the window [−100 μm, 100 μm] at $t=5$ s which is approximately equal to the number of atoms in the generated gap soliton as a function of the final depth of the optical lattice. Initially, there are 500 atoms in the condensate. Dashed line corresponds to the case of a constant lattice depth, and the solid line to the case of the adiabatic reduction of the lattice potential from $\varepsilon=8E_{\mathrm{recoil}}$ to the final depth during the first 500 ms.

IV. COUPLED-MODE THEORY OF SELF-TRAPPING

In this section, we introduce a simple analytical model that allows us to get a deeper insight into the physics of the soliton generation and self-trapping in nonlinear systems with repulsive interaction. Such a model describes the dynamics in the momentum space, but it is restricted by the first Brillouin zone of the band-gap spectrum.

To derive the model, we decompose the condensate wave function in the basis of the Bloch functions and then show the spontaneous migration toward the region of the negative effective mass.

Before the derivation, we introduce the dimensionless variables $z'=z/d$, $t'=t\omega$, $\Psi'=\Psi\sqrt{d/N}$, where $\omega=\hbar/(md^2)$ and N is the number of atoms, and define $g=4\pi dNa_{1\mathrm{D}}$ and $\varepsilon'=\varepsilon/(\hbar\omega)$.

First, we omit the primes for simplicity and apply the Fourier transform of the one-dimensional rescaled model

$$i\frac{\partial\Psi(k,t)}{\partial t}=\frac{k^2}{2}\Psi(k,t)-\frac{\varepsilon}{4}[\Psi(k-2\pi,t)+\Psi(k+2\pi,t)]+\frac{g}{2\pi}\int\int_{-\infty}^{+\infty}\Psi(k_1,t)\Psi^*(k_2,t)\Psi(k-k_1+k_2,t)dk_1dk_2.$$

For the first Brillouin zone, i.e., $|k'|<\pi$, we define the Bloch functions $u(k,k')$ of energy $E(k')$ satisfying

$$E(k')u(k,k')=\frac{k^2}{2}u(k,k')-\frac{\varepsilon}{4}[u(k-2\pi,k')+u(k+2\pi,k')],$$

with normalization condition $\int u(k,k_1')u^*(k,k_2')dk=\delta(k_1'-k_2')$. According to our assumption mentioned above we can decompose the wave function $\Psi(k,t)$ into these states,

$$\Psi(k,t)=\int_{-\pi}^{\pi}\Phi(k',t)u(k,k')dk',$$

and obtain the equation for the amplitudes $\Phi(k',t)$,

$$i\frac{\partial\Phi(k',t)}{\partial t}=E(k')\Phi(k',t)+\frac{g}{2\pi}\int\int\int_{-\pi}^{\pi}\Phi(k_1',t)\Phi^*(k_2',t)\Phi(k_3',t)dk_1'dk_2'dk_3'\times\int\int\int_{-\infty}^{+\infty}u^*(k_0,k')u(k_1,k_1')u^*(k_2,k_2')\times u(k_0-k_1+k_2,k_3')dk_0dk_1dk_2.$$

For a weak lattice we assume that $u(k,k')\approx\delta(k-k')$; this approximation works well everywhere except the regions close to the band edge. Using this assumption, we obtain

$$i\frac{\partial\Phi(k,t)}{\partial t}=E(k)\Phi(k,t)+\frac{g}{2\pi}\int\int_{-\pi}^{\pi}\Phi(k_1,t)\Phi^*(k_2,t)\times\Phi(k-k_1+k_2,t)dk_1dk_2. \quad (3)$$

We further simplify the dynamics by introducing a two-mode approximation; namely, we assume that to the first order our wave function consists of constant and modulated parts $\Phi(k,t)=[a(t)+\sqrt{2}b(t)\cos(k)]/\sqrt{2\pi}$, $E(k)=E_0+E_1\cos(k)$, where $E_1<0$ and $|a|^2+|b|^2=1$. Equation (3) yields

$$\frac{da}{dt}=-\frac{i}{\sqrt{2}}E_1b-ig|a|^2a,$$

$$\frac{db}{dt}=-\frac{i}{\sqrt{2}}E_1a-\frac{i}{2}g|b|^2b. \quad (4)$$

After substituting

$$a(t)=\sqrt{\frac{1-z(t)}{2}}\exp[i\phi_0(t)],$$

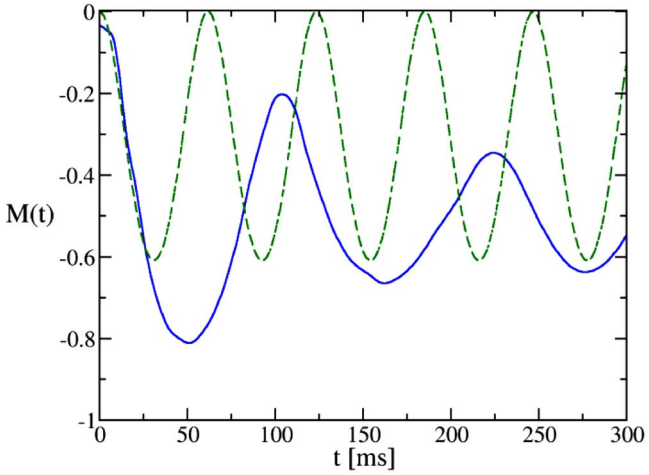

FIG. 9. (Color online) Evolution of the parameter $M(t)$ above the threshold for soliton formation ($N=500$ atoms), corresponding to Fig. 1(c). Solid line shows the results of the one-dimensional GPE model, and dashed line shows results of the coupled-mode model, Eqs. (4).

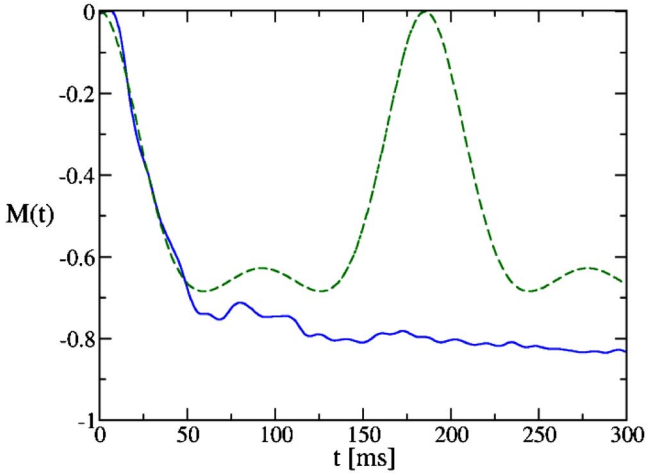

FIG. 10. (Color online) As in Fig. 9, but in the case of $N=200$ atoms; see Fig. 1(b).

$$b(t) = \sqrt{\frac{1+z(t)}{2}}\exp\{i[\phi_0(t) - \phi(t)]\},$$

we obtain the asymmetric Josephson junction equations

$$\frac{d\phi}{dt} = \frac{z}{\sqrt{1-z^2}}\cos\phi + \Lambda\left(z - \frac{1}{3}\right),$$

$$\frac{dz}{dt} = -\sqrt{1-z^2}\sin\phi,$$

where we introduce $\Lambda = 3g/(4\sqrt{2}|E_1|)$, and use the rescaled time $t_{\text{new}} = \sqrt{2}|E_1|t$. To describe the migration of waves from the region of normal to anomalous diffraction, we introduce the quantity $M(t)$, which stands for a difference between the population of atoms in the normal (central) and anomalous (outer) regions of the Brillouin zone,

$$M(t) = \int_{-\pi/2}^{\pi/2} |\Phi|^2 dk - \left(\int_{-\pi}^{-\pi/2} |\Phi|^2 dk + \int_{\pi/2}^{\pi} |\Phi|^2 dk\right)$$
$$= \frac{4\sqrt{2}}{\pi}\,\mathrm{Re}(ab^*) = \frac{2\sqrt{2}}{\pi}\sqrt{1-z^2}\cos\phi.$$

For $M>0$, the condensate is composed mostly of matter waves from the normal diffraction region, and for $M<0$ of the matter waves from the anomalous diffraction region. The temporal derivative of M can be expressed as

$$\frac{dM}{dt} = \frac{2\sqrt{2}}{\pi}\Lambda\left(z - \frac{1}{3}\right)\frac{dz}{dt}. \tag{5}$$

To apply this equation for describing the dynamics of soliton generation, we assume that at $t=0$ the condensate is in the ground state of a single lattice site. In this state, the first band is populated approximately uniformly with a constant phase, so that $a=1$ and $b=0$ and, consequently, $z=-1$ and $M(0)=0$. Since z cannot be smaller than -1, z will grow in time and from Eq. (5) we see that $M(t)$ will initially decrease for a repulsive condensate ($\Lambda>0$). Hence the matter waves will change their state, migrating to the regions of negative effective mass, allowing the gap soliton to be formed.

This general picture has been confirmed by direct numerical simulations of both the full Gross-Pitaevskii equation (GPE) and our simplified coupled-mode model, as shown in Figs. 9 and 10. In Fig. 9 we present a comparison of the parameter $M(t)$ calculated from the one-dimensional GPE and Eq. (4) for the case when the soliton is formed (500 atoms in the initial condensate) and Fig. 10 corresponds to the case below the threshold of gap soliton formation. In both cases the initial dynamics is similar and well described by our simple model. However, the nonlinear dynamics observed in the simulations of the full model is more complicated because the energy exchange between the two major modes is accompanied by excitation of other modes in the system not taken into account by our simplified two-mode approximation. In the results obtained for the full model, this effect is observed as an effective damping of the oscillations.

V. CONCLUSIONS

We have revealed that the generation of matter-wave gap solitons can be easier than expected. We propose and demonstrate numerically two generation schemes in which a robust, long-lived stationary wave packet in the form of a matter-wave gap soliton is created in a repulsive Bose-Einstein condensate placed in a one-dimensional optical lattice. The suggested generation method looks simple and efficient, and it relies on a relaxation of the initial distribution of atoms to the appropriate soliton state. For this scheme, the lifetime of the final state is limited only by the lifetime of the condensate. We presented a simple theoretical model to illustrate how the generation method works.

ACKNOWLEDGMENTS

M.M. acknowledges support from the KBN Grant No. 2P03 B4325 and the Foundation for Polish Science. M.T.

was supported by the Polish Ministry of Scientific Research and Information Technology under Grant No. PBZ MIN-008/P03. The work of Y.K. has been supported by the Australian Research Council through the Centre of Excellence Program; Y.K. thanks Elena Ostrovskaya and Tristram Alexander for useful discussions.

[1] Yu. S. Kivshar and G. P. Agrawal, *Optical Solitons: From Fibers to Photonic Crystals* (Academic Press, San Diego, 2003).
[2] L. Khaykovich, F. Schreck, G. Ferrari, T. Bourde, J. Cubizolles, L. D. Carr, Y. Castin, and C. Salomon, Science **296**, 1290 (2002).
[3] K. E. Strecker, G. B. Partridge, A. G. Truscott, and R. G. Hulet, Nature (London) **417**, 150 (2002).
[4] D. N. Christodoulides, F. Lederer, and Y. Silberberg, Nature (London) **424**, 817 (2003).
[5] E. A. Ostrovskaya and Yu. S. Kivshar, Phys. Rev. Lett. **90**, 160407 (2003).
[6] E. A. Ostrovskaya and Yu. S. Kivshar, Opt. Express **12**, 19 (2004).
[7] H. S. Eisenberg, Y. Silberberg, R. Morandotti, and J. S. Aitchison, Phys. Rev. Lett. **85**, 1863 (2000).
[8] J. W. Fleischer, M. Segev, N. K. Efremidis, and D. N. Christodoulides, Nature (London) **422**, 147 (2003).
[9] A. A. Sukhorukov, D. Neshev, W. Krolikowski, and Yu. S. Kivshar, Phys. Rev. Lett. **92**, 093901 (2004).
[10] Yu. S. Kivshar, Opt. Lett. **18**, 1147 (1993).
[11] M. Matuszewski, C. R. Rosberg, D. N. Neshev, A. A. Sukhorukov, A. Mitchell, M. Trippenbach, M. W. Austin, W. Krolikowski, and Yu. S. Kivshar, Opt. Express **14**, 254 (2006).
[12] B. Eiermann, Th. Anker, M. Albiez, M. Taglieber, P. Treutlein, K.-P. Marzlin, and M. K. Oberthaler, Phys. Rev. Lett. **92**, 230401 (2004).
[13] S. Burger, F. S. Cataliotti, C. Fort, F. Minardi, M. Inguscio, M. L. Chiofalo, and M. P. Tosi, Phys. Rev. Lett. **86**, 4447 (2001).
[14] A. Görlitz, J. M. Vogels, A. E. Leanhardt, C. Raman, T. L. Gustavson, J. R. Abo-Shaeer, A. P. Chikkatur, S. Gupta, S. Inouye, T. Rosenband, and W. Ketterle, Phys. Rev. Lett. **87**, 130402 (2001).
[15] K. M. Hilligsøe, M. K. Oberthaler, and K.-P. Marzlin, Phys. Rev. A **66**, 063605 (2002).
[16] D. Neshev, A. A. Sukhorukov, B. Hanna, W. Krolikowski, and Yu. S. Kivshar, Phys. Rev. Lett. **93**, 083905 (2004).
[17] P. J. Y. Louis, E. A. Ostrovskaya, C. M. Savage, and Yu. S. Kivshar, Phys. Rev. A **67**, 013602 (2003); N. K. Efremidis and D. N. Christodoulides, *ibid.* **67**, 063608 (2003).
[18] V. Ahufinger, A. Sanpera, P. Pedri, L. Santos, and M. Lewenstein, Phys. Rev. A **69**, 053604 (2004); B. J. Dabrowska, E. A. Ostrovskaya, and Y. S. Kivshar, J. Opt. B: Quantum Semiclassical Opt. **6**, 423 (2004).